Reactions of Alpha Particles with Tin-124*

R. L. Hahn† and J. M. Miller
Chemistry Department, Columbia University, New York, New York, and Chemistry Department, Brookhaven National Laboratory, Upton, New York

(Received August 1, 1961)

The excitation functions for the (α,n), (α,p), (α,pn), $(\alpha,2pn)$, $(\alpha,3n)$, and $(\alpha,\alpha n)$ reactions of Sn^{124} have been determined with alpha particles from 13–42 Mev of excitation energy. Cross sections for the production of the isomers of Te^{127}, Sb^{126}, Sn^{125}, and Sn^{123} are also presented. Reactions in which there is only neutron emission predominate: the maximum cross sections for (α,n) and $(\alpha,3n)$ (metastable state) are 0.161 barn at 18 Mev of excitation and 1.18 barn at 36 Mev, respectively. The (α,p) has its maximum of 0.017 barn at 28 Mev, while the largest cross section obtained for the $(\alpha,\alpha n)$ reaction is 0.056 barn at 42 Mev. The results are discussed in terms of the statistical theory of nuclear reactions. A satisfactory fit to the (α,n) and (α,p) data is obtained for $r_0=1.7$ fermis and $a=1.6$ Mev^{-1}. However, both excitation functions exhibit high energy tails not predicted by the theory. An evaporation calculation using $a=1.6$ Mev^{-1} yields cross sections of proper magnitude for the $(\alpha,\alpha n)$ reaction; but the shape of the experimental curve is not indicative of compound nuclear processes.

I. INTRODUCTION

In terms of the statistical theory of nuclear reactions, the investigation of the excitation functions of a nucleus with high Z, and with a large neutron excess, is of interest because of the effects that the Coulomb barrier and the neutron excess will have on particle emission. The appreciable Coulomb barrier and the difference in the binding energies of neutrons and protons for such a nucleus will favor predominant emission of neutrons when the nucleus is excited above the threshold for particle emission.

This situation can be investigated theoretically by means of the well-known fundamental equation of evaporation theory[1] for the probability per unit time, $W(\epsilon)$, that a particle is emitted with kinetic energy between ϵ and $\epsilon+d\epsilon$,

$$W(\epsilon)d\epsilon \propto \sigma(\epsilon)\epsilon[\rho(U_B)/\rho(U_C)]d\epsilon. \quad (1)$$

$\sigma(\epsilon)$ is the cross section for the inverse process, $\rho(U)$ is the nuclear level density at excitation U, and C and B refer to the initial and residual nucleus. $\rho(U)$ is usually obtained from the model of a Fermi degenerate gas,

$$\rho(U)=C\exp 2(aU)^{\frac{1}{2}}, \quad (2)$$

where C and a are constants.[1] Upon integrating Eq. (1) to get the total emission rate for a given particle, one essentially finds $W(u)\propto g(u)f(u)$, where g is a polynomial if $\sigma(\epsilon)\propto(1-kV/\epsilon)$, f is an exponential function, and $u=(U_C-S-kV-\delta)$. Here U_C is the excitation energy of initial nucleus C; S, the separation energy of the particle from C; kV, the Coulomb barrier approximately corrected for tunneling; and δ, the energy associated with symmetry and shell effects.[2] The theory thus predicts a particular functional dependence on these quantities which then can be compared with experiment. An important point is that by means of this comparison, one can obtain a value for a, the parameter in the level density expression. This value and its expected proportionality to A can then be compared with the values determined with other mass number targets.

The above considerations have been employed in the study of the compound nucleus Te^{128}, formed in the alpha-particle irradiation of Sn^{124}. (Among the excitation functions determined by alpha bombardments for elements with $100<A$ are those for Ag^{109} by Bleuler *et al.*,[3] Ag^{107} by Porges,[4] In by Temmer,[5] Pb^{206} by John,[6] and Ba^{138} by Caretto and Friedlander.[7]) Moreover, because the Coulomb barrier is not prohibitively high, one may experimentally examine such charged particle reactions as the (α,p), (α,pn), and $(\alpha,2pn)$ and their relationship to the (α,xn) reactions. Also, the $(\alpha,\alpha n)$ reactions, generally considered to proceed through a non-compound-nucleus mechanism, can be investigated. Unfortunately, the $(\alpha,2n)$, $(\alpha,2p)$, $(\alpha,\alpha 2n)$, and ground state isomer of the $(\alpha,3n)$ products of Sn^{124} are stable and so are not detected in this experiment. Nevertheless, a limited comparison with the total reaction cross section as derived from continuum theory[8] or from the optical model[9] can be obtained.

II. EXPERIMENTAL PROCEDURES

Bombardments

The irradiations were performed in the external alpha-particle beam of the Brookhaven 60-in. cyclotron. Several targets were irradiated concurrently by means of the stacked foil method. Aluminum foils

* Research performed under the auspices of the U. S. Atomic Energy Commission.

† This work was submitted in partial fulfillment of the requirements for the degree of Doctor of Philosophy in the Faculty of Pure Science of Columbia University.

[1] V. F. Weisskopf, Phys. Rev. **52**, 295 (1937).

[2] H. Hurwitz and H. A. Bethe, Phys. Rev. **81**, 898 (1951).

[3] E. Bleuler, A. K. Stebbins, and D. J. Tendam, Phys. Rev. **90**, 460 (1953).

[4] K. G. Porges, Phys. Rev. **101**, 225 (1956).

[5] G. M. Temmer, Phys. Rev. **76**, 424 (1949).

[6] W. John, Phys. Rev. **103**, 704 (1956).

[7] A. A. Caretto and G. Friedlander, Phys. Rev. **110**, 1169 (1958).

[8] J. Blatt and V. F. Weisskopf, *Theoretical Nuclear Physics* (John Wiley & Sons, Inc., New York, 1952).

[9] G. Igo, Phys. Rev. **115**, 1665 (1959).

placed between the Sn^{124} targets served both to degrade the energy of the beam and to catch recoil nuclei. Interpolated values of the range-energy relation for alpha particles in tin were obtained from the data on the regular variation of range with Z, the nuclear charge of the absorbing material, presented in Aron *et al.*[10]; their curves for aluminum were also used in determining the energy degradation of the beam. The energy of the incident beam was monitored by either measuring the degradation of energy through aluminum absorbers[11] or by measuring the gross activity of copper foils placed in the stack.[12] A calibrated charge integrator attached to the Faraday cup assembly[13] monitored the beam intensity.

The targets were 0.0005-in. foils of enriched Sn^{124} which were within 10% of uniform thickness.[14] Emission spectrographic analyses of the foils showed no significant impurities. Mass spectrography revealed the presence of Sn^{122} and Sn^{120}, both of which can lead to products which are also produced from Sn^{124} [the (α,n) reactions of Sn^{124} and Sn^{120} lead to tellurium nuclei which cannot be distinguished from each other].

Chemistry

After irradiation, the target was dissolved in $6N$ hydrochloric acid which contained antimony, tellurium carriers, and hydrogen peroxide. The peroxide was boiled off and sulfur dioxide was bubbled into the solution, causing tellurium to precipitate in its elemental form. The sulfur dioxide was boiled off and $7M$ ammonium thiocyanate was added to the remaining solution. The tin thiocyanate was then separated from the antimony by extraction into ethyl ether. Following several purification steps, each element was precipitated and mounted for counting on aluminum cards: tellurium in the form of the element; antimony as the 8-hydroxyquinolate; and tin as the cupferrate. The sample thicknesses were all less than 1 mg/cm^2. In most instances, the antimony activity in the catcher foils was mounted separately and counted as a measure of the loss due to recoil. The aluminum catcher was dissolved in $6N$ hydrochloric acid containing antimony, tellurium, and tin carriers and hydrogen peroxide; a procedure similar to that for the target was then followed. After the various activities were measured, spectrophotometric analyses were performed to determine the chemical yield of each sample.

Counting

Most of the samples were assayed by means of their beta radiation. The observed half-lives compared to within 3% of those in the literature except in the case of Sb^{126} which has a listed half-life of 6.2 days.[15,16] A Sb^{126} sample accordingly was prepared and the predominant 0.42- and 0.68-Mev gamma rays counted over a period of two months with a 3×3-in. NaI(Tl) crystal in conjunction with a hundred-channel pulse height analyzer. The observed mean half-life for the gammas was 12.2±0.1 days.

The total efficiencies of the beta counters were determined for the various isotopes with the aid of calibrated samples. In all these cases, variations in the self-absorption of beta-particles for different samples of the same isotope were neglected because each sample's thickness was less than 1% of the beta range[17]; the efficiency factor determined for the calibrated isotopic sample was used for all the samples of that isotope.

(1) Sn^{123}, 41.5-min. isomer: The 0.153-Mev gamma was counted with a 3×3-in. NaI(Tl) crystal for which the variation of intrinsic peak efficiency with gamma energy had been previously estimated with the aid of samples from the Bureau of Standards.[18] The samples were also counted in a beta-proportional counter to determine the total efficiency for the 1.3-Mev betas. The same efficiency factor was used for the 1.4-Mev beta of 130-day Sn^{123}.

(2) Sn^{125}, 9.7-min. isomer: The 0.33-Mev gamma ray, which occurs in 99.7% of the transitions, was counted in the calibrated scintillation spectrometer. The samples were also counted in a beta-proportional counter and the efficiency factor for the 2-Mev beta determined. This efficiency value was also used for the 2.4-Mev beta of the 9.9-day isomer of Sn^{125}.

(3) Te^{125}: The K x rays were counted with a 2-mm-thick NaI(Tl) crystal under conditions of known geometry. To obtain the disintegration rate, the decay scheme presented by Bowe and Axel,[19] along with their value of 0.82 for the K-shell fluorescence yield w_K, was used. Correction was made for the unconverted 35-kev gamma ray included in the x-ray peak.

(4) Te^{127m}: The K x rays due to the 98.5% isomeric transition were counted in the same arrangement as Te^{125}. The 0.089 gamma was assumed to be completely converted, and K/L was taken to be 0.75.[20] $w_K=0.855$ was used.[21]

[10] W. A. Aron, B. G. Hoffman, and F. C. Williams, Atomic Energy Commission Rept. No. 663, 1949 (unpublished).
[11] J. R. Grover, B. M. Foreman, Jr., B. D. Pate, C. P. Baker, and J. Hudis, Brookhaven National Laboratory Rept. BNL-654, 1960 (unpublished).
[12] N. T. Porile and D. L. Morrison, Phys. Rev. **116**, 1193 (1959).
[13] S. Amiel and N. T. Porile, Rev. Sci. Instr. **29**, 1112 (1958).
[14] Sn^{124} foils were obtained from Isotopes Division, Oak Ridge National Laboratory.
[15] H. E. Bosch, Bull. Am. Phys. Soc. 4, 374 (1959), reports half-life of 11 days.
[16] H. E. Bosch (private communication) reports half-life of 12.6 days.
[17] A. T. Nelms, Natl. Bur. Standards Circ. No. **577**, 1956 (unpublished).
[18] B. M. Foreman, Jr. (private communication).
[19] J. C. Bowe and P. Axel, Phys. Rev. **85**, 858 (1952).
[20] A. C. Helmholz, Phys. Rev. **60**, 415 (1941).
[21] A. H. Wapstra, C. J. Nijgh and R. Van Lieshout, *Nuclear Spectroscopy Tables* (North-Holland Publishing Company, Amsterdam, 1959).

(5) Te^{127}: By determining the total number of K x rays from an equilibrium mixture of Te^{127} and Te^{127m}, and counting the sample in the beta counter, the total efficiency for the 99% 0.7-Mev beta transition of Te^{127} was determined. Aluminum absorbers were used to correct for the effect of conversion electrons in the beta counter.

(6) Sb^{127}: Beta particles were counted until the 92-hr Sb^{127} had completely decayed to Te^{127m}. The K x rays were then counted absolutely and the disintegration rate of parent Sb^{127} calculated. The fraction of Sb^{127} decaying to Te^{127m} was taken to be 0.22.[22]

(7) Sb^{126}: For both the 12.2-day and 18.7-min. isomers the 0.68-Mev gamma ray was counted in the calibrated scintillation counter. Since the decay schemes of these isomers are not known, it was assumed in each case that the number of 0.68-Mev gammas per unit time was equivalent to the nuclear disintegration rate. This assumption causes each cross section reported herein for Sb^{126} to be a lower limit for the (α,pn) reaction.

III. RESULTS

The excitation functions for the long-lived isotopes were obtained from four separate bombardments while 17 irradiations provided the data for the short-lived samples. Errors in the cross-section determinations arise in the main from the determination of the counting efficiencies. For the Te^{125} and Te^{127m} samples in which the x rays were counted in a well-defined system, the efficiency errors are estimated to be ~8%. For the other samples, the uncertainty in the gamma efficiencies plus the error in beta-counter efficiency due to the neglect of scattering effects for the individual samples lead to a cumulative error in the efficiency of ~15%. Other experimental uncertainties include those owing to the statistical fluctuations in the counting rates and to decay curve analyses (3%), to chemical yield determinations (3%), and to the values used for branching ratios and conversion coefficients. Thus the uncertainty in the cross sections of the beta-emitting samples is ~20%, while for the samples of Te^{125} and Te^{127m}, the stated errors are ~15%. A possible systematic error in the cross sections for the (α,n) reactions exists because of other tin isotopes present in the target foils. The products of the (α,n) reactions of Sn^{120} and Sn^{122} can be distinguished from Te^{127m} only with extreme difficulty. Thus, as is seen from Table I, which presents the atomic percent of the tin isotopes of interest in the target, the measured (α,n) reaction leading to Te^{127m} may be high by as much as 6%. Because of the method used to determine the disintegration rate of Te^{127g}, the ground state excitation function may also contain this systematic error.

TABLE I. Composition of targets.[a]

Isotope	Foil "A" (atom %)	Foil "B" (atom %)
Sn^{120}	3.06	1.2
Sn^{122}	2.78	1.2
Sn^{124}	90.3	96.0

[a] Two sets of foils were used in the irradiations; they are designated as foils "A" and "B". For all excitation functions which were measured, the data from foil "A" are in good agreement with those from foil "B".

[22] A. C. Pappas, Massachusetts Institute of Technology Laboratory for Nuclear Science Technical Report 63 (unpublished).

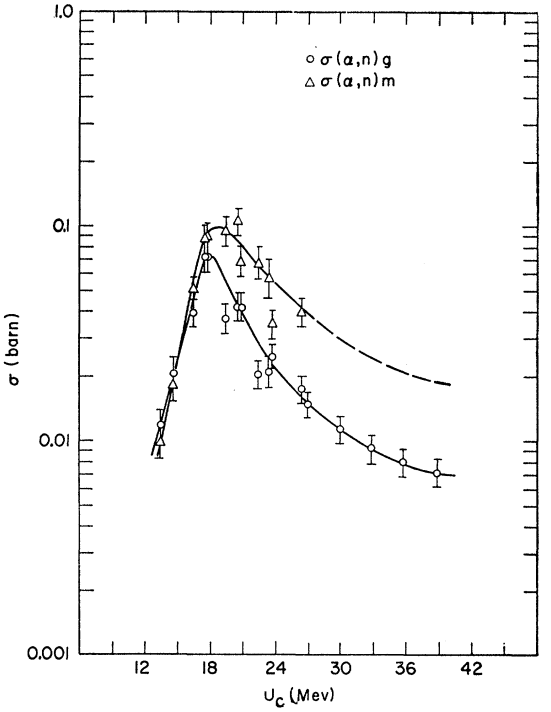

FIG. 1. Excitation functions for the isomers of the (α,n) products. ---, extrapolated from isomer ratio.

Recoil losses measured for the antimony fractions of the catcher foils were 1.5% of the total activity for the (α,p) product at the highest energy measured. The recoil losses for the (α,pn) reaction were less than 1%. Corrections for recoil losses that were not experimentally determined were based on the assumption that the momentum distribution of recoiling nuclei after emission of x particles was independent of the nature of the particles; that is, the ratio of recoil losses of (α,xp) to (α,xn) is unity.

The (α,n) excitation function for the isomeric states are shown in Fig. 1. Because of the similarity of radiation and half-life between the (α,n) metastable state and the $(\alpha,3n)$ product, the Te^{127m} isomer could not be followed beyond 26 Mev. However, as seen in Fig. 2, the isomer ratio of Te^{127} (spin $I=3/2$) to Te^{127m} ($I=11/2$) seems to approach a limiting factor. This behavior is consistent with that observed for isomers of Mn^{52}, Ag^{106}, and Sr^{85} by Linder and James.[23] Using the asymptotic isomer ratio of 0.375 from Fig. 2, one can

[23] B. Linder and R. A. James, Phys. Rev. 114, 322 (1959).

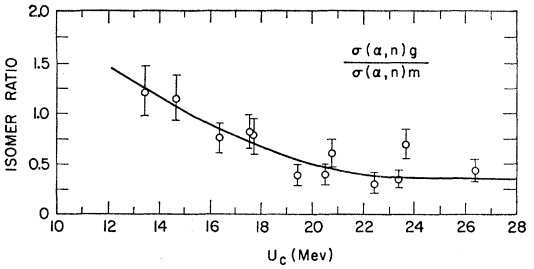

FIG. 2. Isomer ratio for the (α,n) products.

extrapolate the excitation functions for the metastable state and for the total (α,n) reaction to 40 Mev. The maximum value for the (α,n) total curve, as shown in Fig. 3, is 161 mb at 18 Mev; its value at 40 Mev is 26.2 mb.

The excitation function for the (α,p) reaction is also given in Fig. 3. Note that the curve reaches its maximum several Mev above the (α,n) peak. However, at no point in the energy range covered does the (α,p) cross section exceed the (α,n).

Just as the (α,n) reaction is the major portion of the total reaction cross section at energies up to 22 Mev, so does the $(\alpha,3n)$ predominate at the highest energies observed. Its maximum of 1.18 b occurs at an excitation of 36 Mev. The experimentally determined excitation function (solid $(\alpha,3n)$ curve in Fig. 3) is a lower limit to the total $(\alpha,3n)$ reaction for only the isomeric excited state ($I=11/2$) of Te^{125} was measured; the ground state ($I=\frac{1}{2}$) is stable. However, by assuming that the isomer ratio of ground to excited state is equal to $\frac{1}{6}$, the ratio of the spin statistical weights,[23] one can approximately determine the total $(\alpha,3n)$ curve (broken $(\alpha,3n)$ curve in Fig. 3). If the assumed isomer ratio is in error by a factor of 2, the total $(\alpha,3n)$ cross section will be in error by only some 17%.

Average values of the total excitation functions for the $Sn^{124}(\alpha,pn)Sb^{126}$, $Sn^{124}(\alpha,2pn)Sn^{125}$ and $Sn^{124}(\alpha,\alpha n)Sn^{123}$ reactions are also presented in Fig. 3. The data for the isomers of Sb^{126}, Sn^{125}, and Sn^{123} are shown in Figs. 4–6, respectively. It is seen, in contrast to the (α,p) data, that none of these other charged particle excitation functions attain their maximum values in the energy range investigated.

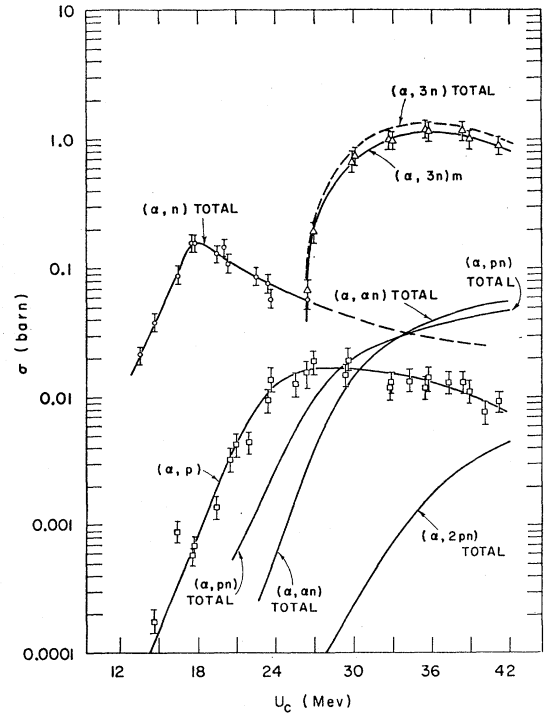

FIG. 3. Excitation functions for the (α,n), (α,p), $(\alpha,3n)$, $(\alpha,\alpha n)$, (α,pn), and $(\alpha,2pn)$ reactions. – – –, extrapolated values based upon isomer ratios.

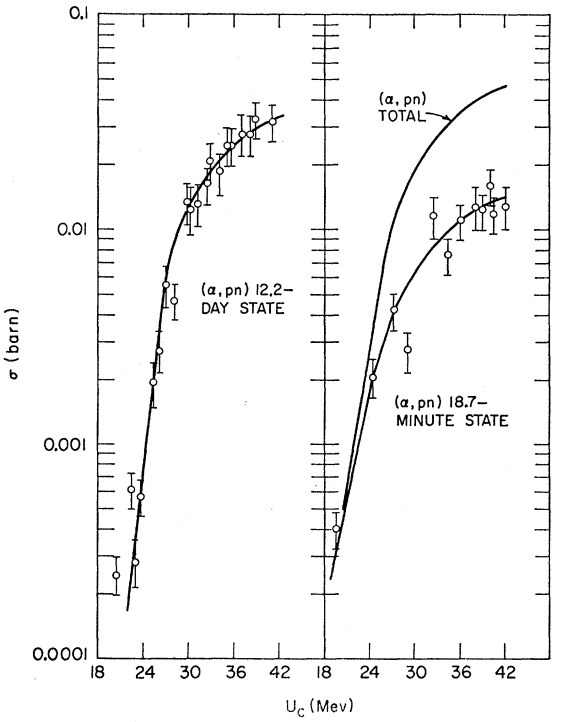

FIG. 4. Excitation functions for the isomers of Sb^{126} produced in the (α,pn) reaction.

It is possible that secondary neutrons produced during the irradiation may lead to an (n,γ) reaction on Sn^{124}, and so contribute to the Sn^{125} cross section. However, one would expect the dependence on energy of the (n,γ) cross section to be much less than that shown in Fig. 5; from the data, one can conclude that the effects due to the (n,γ) reaction are quite small. The contribution of the Sn^{122} impurity to the yield of Sn^{123} via the $(\alpha,2pn)$ reaction may also be neglected; the small value of the $(\alpha,2pn)$ cross section, combined with the few percent of Sn^{122} in the target, contributes less than 1% to the $(\alpha,\alpha n)$ excitation function.

The experimentally determined cross sections and the energies at which they were measured are presented in Table II.

IV. DISCUSSION

The sum of the cross sections observed in this experiment as well as theoretical estimates of the total reaction cross section are plotted versus excitation energy in Fig. 7. In the experimental curve, the "valley" in the region of 18–27 Mev is a result of the fact that the $(\alpha,2n)$ product is stable. At 36 Mev, the experimental curve, including the assumed contribution of the $(\alpha,3n)$ ground state, is a reasonable estimate of the total reaction cross section; from the observed behavior

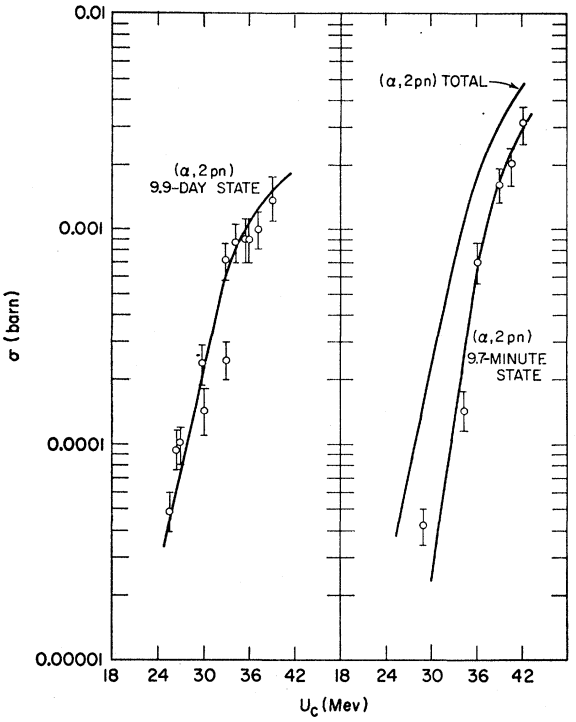

FIG. 5. Excitation functions for the isomers of Sn^{125} produced in the $(\alpha,2pn)$ reaction.

of the $(\alpha,\alpha n)$, (α,pn), and $(\alpha,2pn)$ products, one can infer that the contribution to the total curve of the undetected $(\alpha,\alpha\gamma)$, $(\alpha,\alpha 2n)$, and $(\alpha,2p)$ cross sections is negligible. The missing $(\alpha,2n)$ data prevent one from comparing theory and the experimental curve over an extended range. However, an indication of the comparison can be obtained in the region of 36 Mev.

The broken curves (with large dashes) in Fig. 7 are based upon the approximations to continuum theory given by Dostrovsky *et al.*[24]

$$\sigma_C=\sigma_g(1+c_j)(1-k_jV_j/\epsilon), \qquad (3)$$

where σ_C and σ_g are the capture and geometric cross

[24] I. Dostrovsky, Z. Fraenkel, and G. Friedlander, Phys. Rev. **116**, 683 (1960).

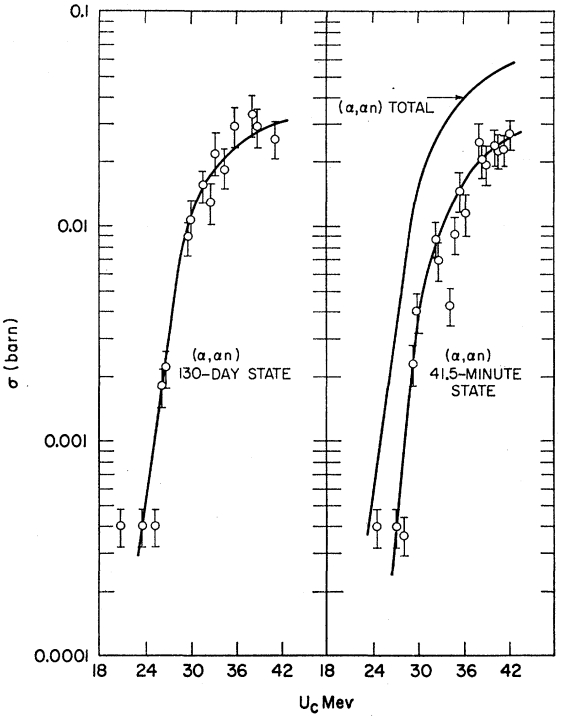

FIG. 6. Excitation functions for the isomers of Sn^{123} produced in the $(\alpha,\alpha n)$ reaction.

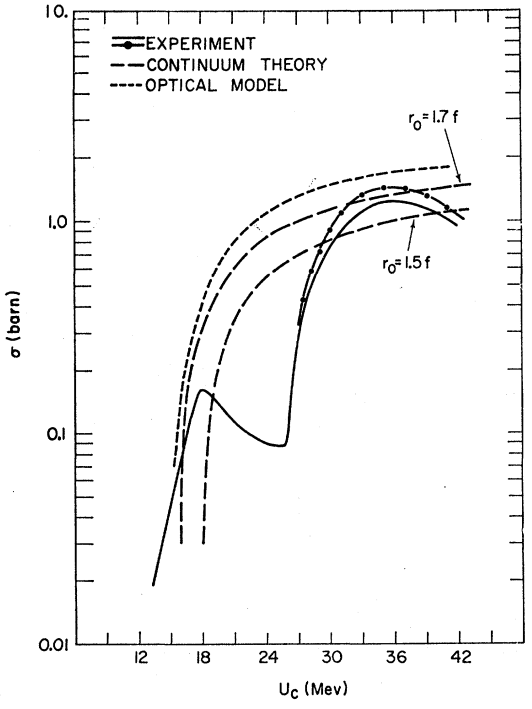

FIG. 7. Total reaction cross section. ——, experimental sum; —·—·—, experimental sum plus assumed contribution of $(\alpha,3n)g$; — — —, calculated from approximation to continuum theory (see Eq. (3)); – – –, calculated from optical model (see reference 9).

TABLE II. Experimental cross sections (millibarns).

Energy	(α,n) g	(α,n) m	(α,p)	(α,pn) (12 day)	(α,pn) (19 min)	$(\alpha,2pn)$ (10 day)	$(\alpha,2pn)$ (10 min)	$(\alpha,3n)$ m	$(\alpha,\alpha n)$ (130 day)	$(\alpha,\alpha n)$ (41 min)
42.04					12.7		3.10			26.7
41.20			9.22	31.5				893	25.3	22.9
40.54					11.7		2.01			22.4
40.20			7.58							
40.06					16.0					24.6
38.91	7.09		11.0	32.8		1.37		1000	29.4	
38.88					12.4		1.64			
38.40			12.9	27.6				1170	33.2	20.8
38.02					12.7					24.9
37.33			13.0	27.5		0.99				
36.15					11.0		0.71			11.6
35.75			14.1	24.4		0.88		1160	29.5	
35.48			11.9	24.4		0.91		1200	18.4	14.7
34.90										9.34
34.38					7.71		0.14			4.44
34.31			13.3	18.4		0.85			21.9	
32.84			13.0	20.7				986	13.1	
32.75			11.9	16.2		0.71		1000	15.6	5.93
32.28					11.4					8.55
31.36				13.0						
30.09	11.4		19.3	12.2		0.14		742	10.7	
29.89			15.0	13.5		0.24		667	8.90	3.98
29.50										2.30
29.01					2.76		0.04			0.36
28.40				4.63						
27.19					4.22					0.41
26.84	14.8		19.2	5.50		0.10		196	2.23	
26.41	17.5	40.0	15.6	2.70		0.09		69.3	1.75	
25.45			12.7	1.91		0.05			0.43	
24.65					2.06					0.44
23.67	24.4	35.0	13.8	0.61					0.37	
23.39	21.0	57.5	9.67	0.28						
22.44	20.6	66.8	4.43	0.56						
20.80	41.9	67.8	4.31						0.40	
20.53	41.9	106	3.29	0.24						
19.74					0.40					
19.43	37.1	94.0	1.39							
17.70	70.9	88.8	0.74							
17.60	71.3	87.3	0.59							
16.46					0.07					
16.44	39.0	51.0	0.89							
14.68	20.5	18.0	0.18							
13.47	11.8	9.77								

sections respectively, and k_jV_j is the Coulomb barrier for particle j, corrected for barrier penetration. In computing the nuclear radius, $R=r_0A^{\frac{1}{3}}$, $r_0=1.5$ and 1.7 fermis were used with the appropriate values of the constants c_j and k_j. In the region of threshold, σ_C deviates most from the experimental data because of the approximate manner in which barrier penetration is treated. At higher energies, a value of $r_0\approx1.7$ fermis is indicated. The results of an optical model computation of the total reaction cross section by Igo[9] are presented as the broken curve (with small dashes) in Fig. 7. At 36 Mev, the fit to the experimental data is within 16%.

Figure 8 presents the ratios of the (α,p) to total (α,n) cross sections. Because the (α,p) reaction does not become appreciable until after the (α,n) has attained its maximum value, the ratio increases very rapidly with increasing excitation until the (α,p) peak is reached. Calculations of the probabilities of neutron and proton evaporation from compound nucleus Te^{128} were based upon a treatment of Houck and Miller.[25]

[25] F. S. Houck and J. M. Miller, Phys. Rev. **123**, 231 (1961).

Beginning with Eq. (1), the integrated probability per unit time for particle emission is calculated for three cases:

(1) If the nucleus is excited above the energy δ, one uses the exponential dependence of the level density,

$$\rho(\epsilon_m-\epsilon)=C\exp[2a^{\frac{1}{2}}(\epsilon_m-\epsilon-\delta)^{\frac{1}{2}}], \quad (4)$$

where $\epsilon_m=U_C-S$. (By inserting δ in the level density expression, one corrects for pairing and shell effects by counting the excitation energy from a characteristic level, displaced upward from the ground state.[24])

(2) In examining emission from levels between the ground state and the characteristic level, Eq. (4) cannot be used since $0\leq\epsilon_m-\epsilon\leq\delta$. Instead, a constant level density is assumed, $\rho(\epsilon_m-\epsilon)=C$.

(3) The above considerations lead to W_i, the total emission rate from a nucleus with excitation between 0 and (U_C-S) Mev. W_i is equivalent to the single-particle emission rate, W_i', below the threshold for evaporation of a second particle. If the excitation is

above this threshold, one may calculate W_i' by requiring that only one emission is energetically allowed: $\epsilon_m - S' \leq \epsilon \leq \epsilon_m$, where S' is the separation energy of the most loosely bound particle in the residual nucleus.

The calculations were performed on an IBM 610 computer. The inverse cross section used for charged particles was given by Eq. (3); for neutrons, $\sigma_C \sigma_g \alpha(1+\beta/\epsilon)$ was used where α and β are constants.[24] The advantage in using these approximate forms for σ_C lies in the fact that the computation can then be carried out in closed form. Separation energies were taken from the literature[26]; these values appear in Table III. The constants a and δ were treated as parameters. Initial values of δ for residual nuclei Sb^{127} and Te^{127} were taken from Cameron.[27] The ratio W_p'/W_n' is plotted in Fig. 8 for $r_0=1.7$ fermis and three values of a. It was found that in the region where the experimental ratio increases rapidly, changing the value of a alters the slope of the computed curve significantly. To move the curve laterally with only a small change in slope, one must change the value of δ. The curves presented are for $\delta_p(Sb^{127})=1.94$ Mev and $\delta_n(Te^{127})=1.04$ Mev, while Cameron's respective values are 0.94 and 1.04 Mev. Using the latter values results in the W_p'/W_n' ratio being too large; by increasing δ_p, one inhibits the proton emission and obtains a satisfactory fit with experiment from 18–24 Mev for $a=1.6$ Mev^{-1}. A value of $a=3.2$ seems reasonable also, but it is evident that still larger values give poor fits to the data. Satisfactory agreement was also obtained using $a=1.6$ Mev^{-1}, $r_0=1.5$ fermis, $\delta_p=0.74$ Mev and $\delta_n(Te^{127})=1.04$ Mev, while Cameron's respective values are 0.94 and 1.04 Mev. Using the latter values results in the W_p'/W_n' ratio being too large; by increasing δ_p, one inhibits the proton emission and obtains a satisfactory fit with experiment from 18–24 Mev for $a=1.6$ Mev^{-1}. A value of $a=3.2$ seems reasonable also, but it is evident that still larger values give poor fits to the data. Satisfactory agreement was also obtained using $a=1.6$ Mev^{-1}, $r_0=1.5$ fermis, $\delta_p=0.74$ Mev, and $\delta_n=1.04$ Mev, reflecting the inhibition of proton emission by the increase in the Coulomb barrier due to a smaller radius. It is of interest that the experimental ratio increases by a factor ~ 100 for an energy increment of 6 Mev. The fact that the particular functional form of the emission rate predicted by compound nucleus theory succeeds in fitting the data in the region of this rapid change is of significance.

TABLE III. Separation energies (Mev).[26] (S, S', and S'' are the respective separation energies for the initial nucleus, the residual nucleus, and the nucleus remaining after a particle has been emitted from the residual nucleus.)

Initial nucleus	Emitted particle	S	Residual nucleus	S'	S''
Te^{128}	n	8.5	Te^{127}	6.38	
	p	9.3	Sb^{127}	8.6	
	α	2.14	Sn^{124}	8.44	14.3

[26] *Nuclear Data Sheets* (National Academy of Sciences–National Research Council, Washington, D. C., 1959).
[27] A. G. W. Cameron, Can. J. Phys. **36**, 1040 (1958).

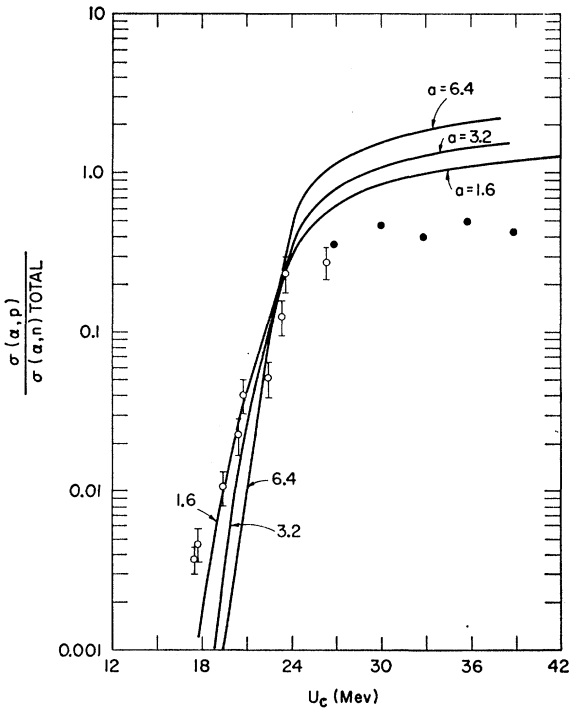

FIG. 8. $\sigma(\alpha,p)/\sigma(\alpha,n)$—total. Open circles are experimental ratios. Closed circles are ratios based upon behavior of the isomer ratio of the (α,n) products. Curves are calculated W_p'/W_n'.

The behavior of the experimental ratio at energies above 24 Mev could not be duplicated by using a set of parameters which gave agreement with the data below 24 Mev. In order to understand this property of the experimental results, the excitation functions for the (α,p) and (α,n) reactions, rather than simply their ratio, were calculated using the same parameters which gave the best fit to the ratio. The basis of the compound nucleus theory is the concept that its formation and decay are independent. Thus

$$\sigma_i = \sigma_C W_i'/\textstyle\sum_j W_j, \tag{5}$$

where σ_C is the cross section for forming the compound nucleus, $\sum_j W_j$ is the sum of emission rates for all particles and σ_i is the cross section for the reaction in which the compound nucleus is formed and particle i is evaporated. $W_i'/\sum_j W_j$ then is the probability that particle i and only particle i is emitted. Values of σ_C were taken from Fig. 7 for $r_0=1.7$ fermis. Using $\sum_j W_j = W_n + W_p$ introduced an error of only a few percent into the computation. The calculated results are compared with experiment in Fig. 9. Use of $a=1.6$ appears preferable to an $a=3.2$. The calculated curves for (α,n) and (α,p) reactions follow the low-energy behavior of the data very satisfactorily. However, the experimental excitation functions exhibit high-energy

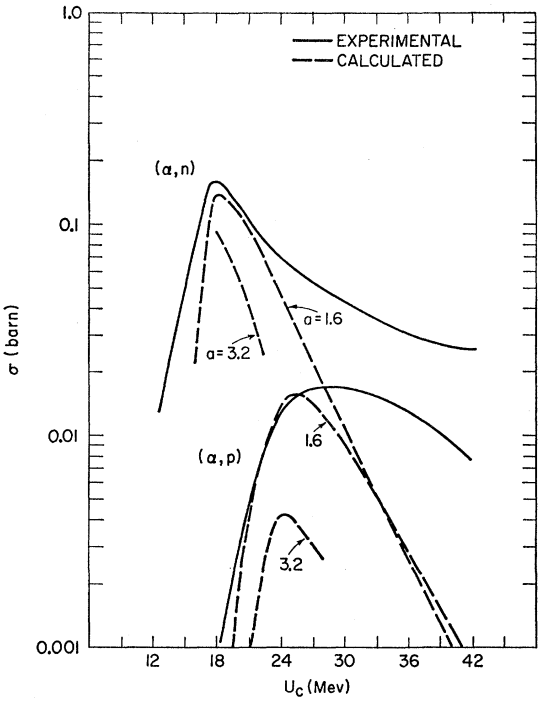

FIG. 9. Experimental and calculated (α,n)—total and (α,p) excitation functions.

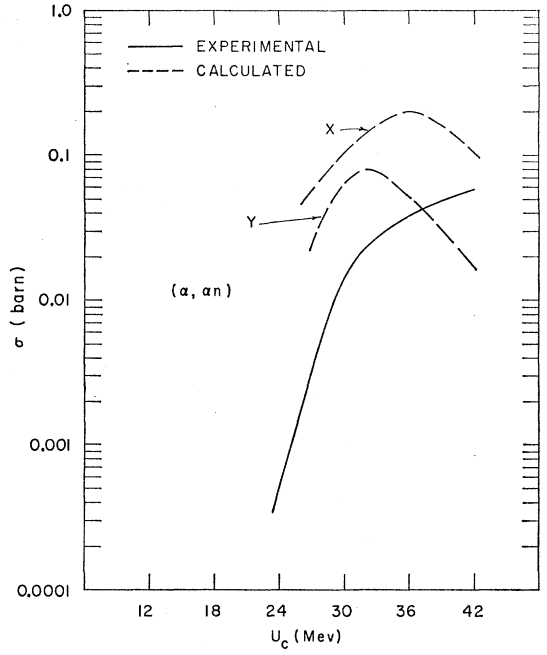

FIG. 10. Experimental and calculated $(\alpha,\alpha n)$ excitation functions. For curve Y: the excitation energy of the final nucleus, U_R, is not greater than the separation energy, S'', of the most loosely bound particle; for curve X: the neutron has ~5-Mev kinetic energy, i.e., $U_R \leq S''-5$.

tails which are quite different from the characteristic rapid decrease of the calculated curves. This behavior has been observed for many excitation functions and is considered a consequence of non-compound-nuclear processes. In evaporation, as a result of the monotonic increase with energy of the total rate of particle emission, the single-particle evaporation probability decreases rapidly above the threshold for multiple particle emission. If direct interactions occur above this threshold, a higher probability of single-particle emission is expected than from the statistical theory because of the greater probability for the emission of high-energy particles which should result from the non-compound processes. It appears, then, that the single-particle emission process is dominated by the mechanism of compound nucleus formation at energies below ≈ 24 Mev. As the energy increases, the fraction of emissions that proceed through non-compound processes appears to increase and exceeds the evaporation contribution above ≈ 30 Mev.

The small value of a that is required for the best fit to the excitation functions is but another example of the anomaly that was pointed out by Igo and Wegner[28]: $a \approx 2$ and independent of mass number is indicated by excitation function results; $a \sim A$, as expected from the Fermi gas model, if often, but not always,[29] indicated when attention is focused upon the energy spectra of emitted particles.

[28] G. Igo and H. E. Wegner, Phys. Rev. **102**, 1364 (1956).
[29] R. M. Eisberg, G. Igo, and H. E. Wegner, Phys. Rev. **100**, 1309 (1955).

The $(\alpha,\alpha \ldots)$ reactions are of considerable interest for they are generally thought to proceed mainly through non-compound processes. Igo[30] determined, for example, in inelastic scattering of 40-Mev alphas from targets such as copper, niobium, silver, and tantalum, that the differential cross sections could not be explained in terms of the statistical theory, except for the very small fraction of scatterings that went in the backward direction. Nevertheless, Dostrovsky *et al.*[24] found in several cases for $A \leqslant 75$ that the shape and magnitude of $(\alpha,\alpha x)$ excitation functions were reproduced moderately well by evaporation theory. It was thus desirable to investigate the behavior of the $Sn^{124}(\alpha,\alpha n)Sn^{123}$ reaction predicted by the theory. In terms of the evaporation calculation discussed above, the $(\alpha,\alpha n)$ excitation function was obtained from the difference of the emission rates for the $[(\alpha,\alpha\gamma)+(\alpha,\alpha n)]$ and $(\alpha,\alpha\gamma)$ processes. The results of the calculations, in which Cameron's δ values were used with $a=1.6$ Mev^{-1} and $r_0=1.7$ fermis, are shown in Fig. 10. Curve Y was obtained by requiring that only an alpha particle and a neutron could be evaporated; the energy, U_R, of the final nucleus could not exceed the binding energy of a third particle, S''. For curve X, the additional condition that the evaporated neutron had ~5 Mev kinetic energy was required; that is, $U_R \leq S''-5$. It is seen that the small value of a that was used yields cross sections whose magnitudes are of the same order

[30] G. Igo, Phys. Rev. **106**, 256 (1957).

as the experimental results. However, the curve computed from evaporation theory, just as in the case of the (α,n) and (α,p) excitation functions, attains its maximum value and then decreases rapidly; in contrast, the experimental curve appears to be just approaching its maximum at 42 Mev. Thus, again it appears that some non-compound nuclear process is in effect in the $(\alpha,\alpha n)$ reaction.

It could well be that the data, although not explicable in terms of the simple evaporation calculation described herein, may fit within the framework of the compound nucleus model. On the other hand, calculation of excitation functions based on some direct-interaction mechanism would be extremely useful in the analysis of the data; unfortunately, no such calculation is available at the present time.

V. CONCLUSIONS

The optical model calculation of the total reaction cross section appears to agree within 16% with the sum of experimental cross sections in the region of 36 Mev. In terms of the approximate form used for the continuum theory cross section, a value of $r_0 \approx 1.7$ fermis is indicated.

The statistical theory of nuclear reactions predicts values for the (α,p) and (α,n) cross sections which are in agreement with the experimental data in the energy range of 18–24 Mev. An $a=1.6$ Mev^{-1} appears to give the most satisfactory fit. However, the high-energy tails of the (α,p) and (α,n) excitation functions cannot be reproduced by the theory. Evaporation calculations of the $(\alpha,\alpha n)$ excitation function, using $a=1.6$, yield excitation functions of the required magnitude; however, the experimental data do not appear to be the result of compound nuclear processes.

ACKNOWLEDGMENTS

Thanks are due to Dr. C. P. Baker and the crew of the 60-in. cyclotron for the irradiations. The aid of the group at the Brookhaven Computer Center is also appreciated. Finally, one of us (R.L.H.) wishes to thank Columbia University for the Westinghouse and Socony-Mobil fellowships granted him during the course of this work.

PHYSICAL REVIEW VOLUME 124, NUMBER 6 DECEMBER 15, 1961

Nuclear Compressibility and Symmetry Energy*

DAVID S. FALK†
Istituto di Fisica dell' Universita, Genova, Italy

AND

LAWRENCE WILETS††
University of Washington, Seattle, Washington

(Received August 10, 1961)

A modification and generalization of the Puff-Martin model for many-fermion systems is employed to calculate nuclear compressibility and symmetry energy in order to provide a practical test of the model and at the same time obtain useful information about these interesting quantities. An alternative, heuristic, derivation of the Puff-Martin equations is presented in order to exhibit the role of the exclusion principle. The condition stated for normal nuclear matter is that the mean binding energy be minimal (with respect to variation of the Fermi momentum) rather than the Puff-Martin condition that the mean binding energy equal the "single particle" energy at the Fermi surface. These two quantities differ from each other by the rearrangement energy, which is found to be 10 Mev. Employing Puff's potential (hard-shell potential plus a separable Yamaguchi potential, acting only in relative S states), satisfactory agreement is obtained with observed binding energy and density. The value of nuclear compressibility, 214 Mev, falls within the wide range of semiempirical values. The symmetry energy coefficient, 43 Mev, is larger, by 40–80%, than those usually quoted in semiempirical mass formulas. However, our value of the symmetry coefficient is the same as that calculated by Brueckner and Gammel in the absence of odd-state forces; they found the coefficient to be reduced to 26 Mev when a more realistic potential, including odd-state contributions, is employed.

I. INTRODUCTION

A RELATIVELY simple procedure for calculating properties of nuclear matter has been devised by Puff and Martin,[1] based upon the formalism of Martin and Schwinger.[2] Their approximation may be arrived at in the following manner: First the two-body problem is solved as a function of energy ("off the energy shell") in the absence of other particles; the center-of-mass and relative motions separate in this case. Then the Fermi sea is filled loosely according to a prescription which satisfies the exclusion principle in an average way. The loose packing is essential, since two-body scattering is allowed to all final states.

* Supported in part by the U. S. Atomic Energy Commission.

† NATO Postdoctoral Fellow. Present address, Departent of Physics, University of Maryland, College Park, Maryland.

†† From August 1961 to August 1962, Senior National Science Foundation Fellow, Weizmann Institute of Science, Rehovoth, Israel.

[1] R. D. Puff and P. C. Martin, Bull. Am. Phys. Soc. **5**, 30 (1960); R. D. Puff, Ann. Phys. **13**, 317 (1961).

[2] P. C. Martin and J. Schwinger, Phys. Rev. **115**, 1342 (1959).